Review of Scientific Instruments

RESEARCH ARTICLE | JULY 05 2023

Initial progress of the magnetic diagnostics of the MAST-U tokamak

D. A. Ryan ; R. Martin; L. Appel; N. B. Ayed; L. Kogan ; A. Kirk ; MAST Upgrade Team

Rev. Sci. Instrum. 94, 073501 (2023)
https://doi.org/10.1063/5.0156334

Review of Scientific Instruments ARTICLE pubs.aip.org/aip/rsi

Initial progress of the magnetic diagnostics of the MAST-U tokamak

Cite as: Rev. Sci. Instrum. 94, 073501 (2023); doi: 10.1063/5.0156334
Submitted: 28 April 2023 • Accepted: 15 June 2023 •
Published Online: 5 July 2023

D. A. Ryan,[a] R. Martin, L. Appel, N. B. Ayed, L. Kogan, A. Kirk, and MAST Upgrade Team[b]

AFFILIATIONS

UKAEA, Abingdon, United Kingdom

[a]Author to whom correspondence should be addressed: David.Ryan@ukaea.uk
[b]See authorlist of J. R. Harrison *et al.* Nuclear Fusion **59**, 112011 (2019).

ABSTRACT

MAST Upgrade has just begun its third physics campaign in April of 2023. The set of magnetic probes used to diagnose the magnetic field and currents on MAST Upgrade are described, and their calibration procedures are outlined including calculation of uncertainties. The median uncertainty in the calibration factors of the flux loops and pickup coils are calculated as 1.7% and 6.3%. The arrays of installed instability diagnostics are described, and the detection and diagnosis of a specimen MHD mode are demonstrated. Plans for the improvement of the magnetics arrays are outlined.

I. INTRODUCTION

Robust and accurate measurements of currents, magnetic fields and fluxes, are of fundamental importance to the safe and productive operation of any toroidal plasma confinement device. The original MAST tokamak,[1] operating from 2000 to 2013, featured a comprehensive set of magnetic diagnostics,[2] able to accurately diagnose the plasma equilibrium state, as well as a wide variety of high frequency plasma oscillations. Following a thoroughly successful career,[3] in 2013, work commenced to rebuild MAST. The machine now known as MAST Upgrade is designed to address some of the key challenges impeding the development of commercial fusion power: Most notably to further develop high performance plasma scenarios in a low aspect ratio in order to reduce the minimum size and, therefore, cost of a commercial reactor and to address the exhaust challenge by exploring novel plasma exhaust concepts, such as the Super-X divertor. The Super-X divertor required the construction of upper and lower baffled divertor chambers and the addition of 19 new poloidal field coils for enhanced plasma shaping. These additions necessitated a redesign of the magnetic diagnostic system to enable the diagnosis of the plasma state in the divertor chambers and main chamber.

During the initial commissioning phase and first campaign, the new magnetic diagnostics were incrementally brought online, commissioned, and utilized for machine protection and physics studies. The purpose of this paper is to describe the state of the magnetic diagnostics at the start of the second physics campaign (MU02). In Sec. II, the arrays of flux loops, pickup coils, and Rogowski coils used to measure the plasma equilibrium state are described. Section III details the *in situ* calibration procedure and the resulting probe uncertainties are estimated. Section IV describes the current status and future prospects of the MAST Upgrade instability array and demonstrates its use for detecting and diagnosing MHD activity. Section V discusses the near and medium term plans for improvements to the diagnostic, which are to be implemented for subsequent campaigns.

II. EQUILIBRIUM MEASUREMENTS

A. Poloidal flux loops

A poloidal flux loop is a single-core cable arranged as a single turn toroidal loop at a specific poloidal position for measuring the poloidal flux at that point. A time varying flux enclosed by this loop will induce a voltage across the loop ends (known as the loop voltage), which is time integrated in hardware and then digitized. MAST-Upgrade features 102 flux loops, the locations of which are plotted in Fig. 1, and also available on the MAST-U visualizer.[4] The flux loops consist of a single loop of insulated wire with twisted pair tails. The wire used is either 0.3 mm PEEK 1000[5] insulated copper wire or an equivalent 0.5 mm diameter polythermaleze-2000

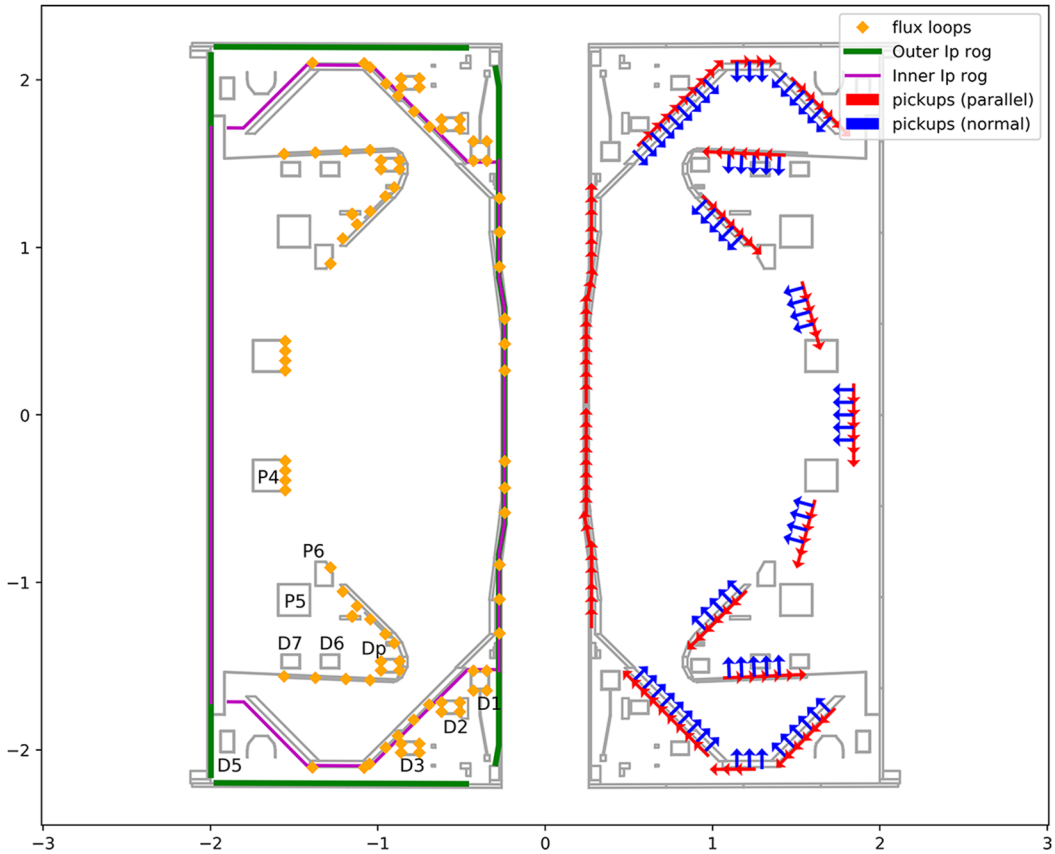

FIG. 1. Sketch of the poloidal arrays of pickup coils and flux loops, as well as paths of the two types of plasma current Rogowski. Note that the toroidally opposite pairs of each plasma current Rogowski, and toroidally opposite pairs of each pickup coil, are not shown for clarity. The UKAEA hosts an interactive browser where the MAST-U geometry may be visualized.[4]

insulated copper wire, threaded through either PEEK 1000 or PTFE tubing (both wire and sleave types have equivalent thermal and electrical performance). The majority of the flux loops are completely protected from the plasma by graphite armor tiles, and thus, the plastic tubing is sufficient for protection and support. However, the graphite tiles protecting the flux loops mounted on the P5 and P6 coils do not provide toroidally contiguous protection; hence, these flux loops are instead threaded through stainless steel tubing.

Flux loops on the D1, D2, D3, and Dp coils (see Fig. 1 and Ref. 4 for coil locations) have the additional purpose of measuring the vertical forces endured by these coils for machine protection. For each of these coils, four flux loops are installed on the rectangular coil cases, one on each corner. By subtracting the upper two signals from the lower two, the radial B field Br can be computed. This summation is performed in real-time in hardware, and the signals are forwarded to the real-time protection system. These signals are then combined with the coil current measurements from external Rogowskis to compute the J × B force on these coils. The uppermost and lowermost flux loops on the center column serve the same purpose as the P1 coil.

As well as flux measurements, the un-integrated loop voltage measurements are also routinely used by tokamak operators. Prior to the third campaign (MU03), due to limited digitizer channels, the loop voltage signals were produced by time differentiating and smoothing the flux measurements in software. Commencing in MU03 direct un-integrated measurements of the center column loop voltages is now also available. By dividing a loop voltage measurement by an effective resistance, the current in toroidal structures adjacent to the flux loop can be deduced, and the vessel current thereby computed. The effective resistances were computed using VALEN 3D as previously reported,[6] and the resulting vessel currents are used in the plasma current calculation (discussed in Sec. III B).

B. Pickup coils

Pickup coils are small multi-turn coils used to measure one vector component of the magnetic field at a single point in (R, Z, ϕ). MAST-U pickup coils consist of a former (of which three different shapes are used, types A, B, and C, enumerated in Table I), around which is wound a 0.366 mm diameter PEEK 1000 insulated copper wire.

TABLE I. The pickup coil types deployed in MAST Upgrade. Figures 1 and 2 show their locations.

Type	Cross section	Winding	NA (m^2)
A	2.9×25.5 mm^2 rect.	Two layers of 71	0.010 5
B	2.2×27 mm^2 rect.	Two layers of 71	0.008 43
C	18 mm diam. circ.	Six layers of 4	0.024 4

These coils are held in mounts of PEEK 1000 (a plastic material with a maximum continuous service temperature of 250 °C, sufficient to withstand vessel bake conditions), and arranged into cassettes of several coils in alternating orientations as shown in Fig. 2, enclosed in a covering of 0.5 mm stainless steel. Unlike the other cassettes, the outboard midplane cassettes are not beneath any graphite vessel armor tiles, so requiring their own 6 mm graphite armor covers. Using the formula below (yielded by inverting the well-known skin depth formula[7]), a wall frequency f_w can be computed, above which signals are attenuated by an electrically conducting covering,

$$f_w = \rho/(\pi\mu_0\mu_r w^2), \tag{1}$$

where ρ, w, and μ_r are the electrical resistivity, covering thickness, and relative permeability of the material, respectively. The 316L steel used in the 0.5 mm cassette covers has $\rho = 0.74\ \mu\Omega$ m and $\mu_r = 1.008$, which yields $f_w = 0.74$ MHz. The graphite armor has a higher resistivity (notoriously varying, but approximated here as 50 $\mu\Omega$ m), but nonetheless has a comparable wall frequency of 0.35 MHz due to its larger thickness. Therefore, in addition to diagnosing the equilibrium state, these pickup coils are able to capture MHD modes of frequencies exceeding 100 kHz, as discussed in Sec. IV of this article. Such cassettes are arranged in arrays proving near complete poloidal coverage with 354 pickups in total measuring the poloidal field, as shown in Figs. 1 and 2 (in practice, a smaller number are typically operating, discussed in Sec. III). The locations and orientations of these coils are available via the MAST-U geometry visualizer.[4]

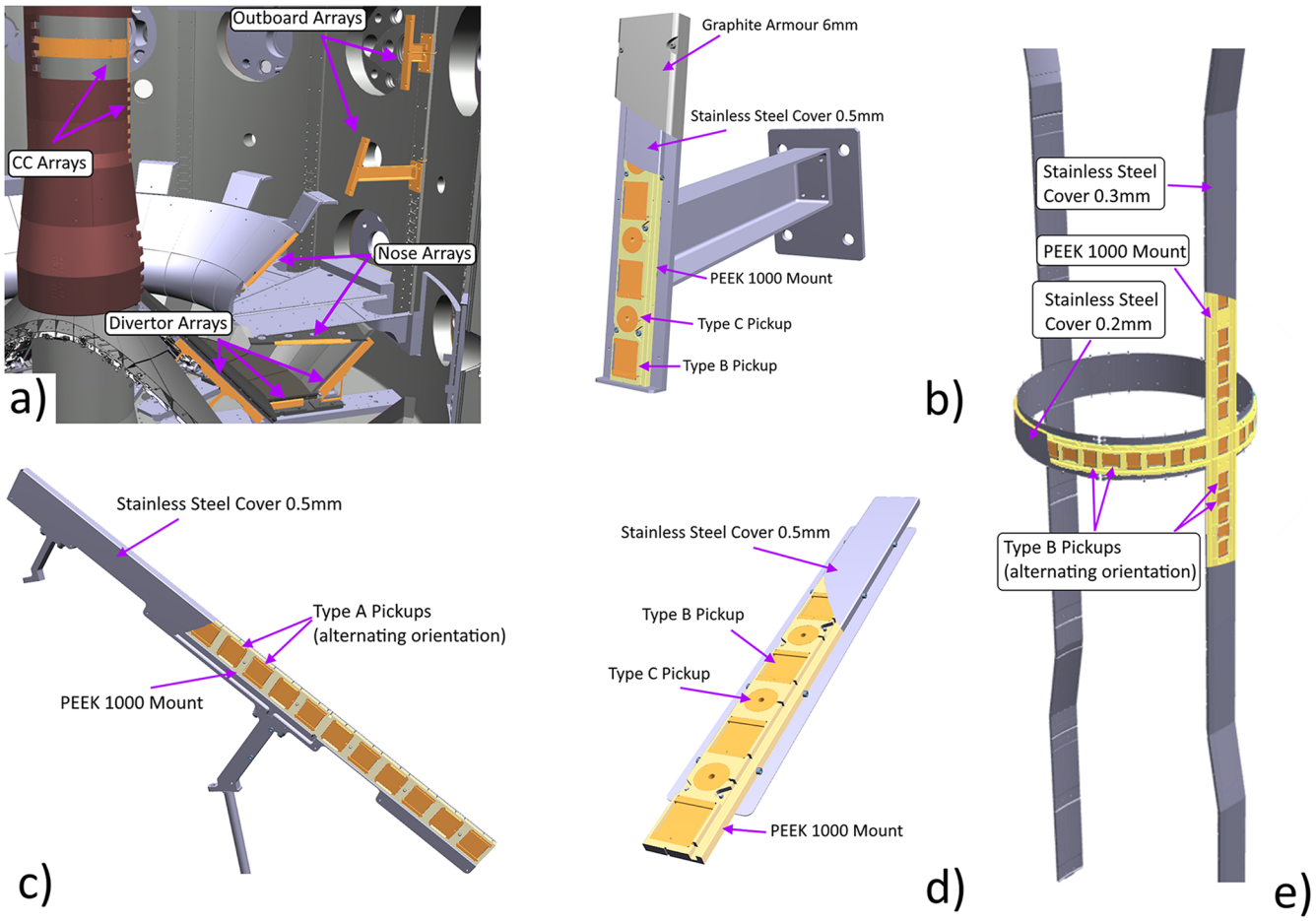

FIG. 2. (a) Sketch of the lower interior of MAST Upgrade, with the pickup coil arrays highlighted. (b) Sketch of an outboard pickup cassette, which is covered by a stainless steel cover and 6 mm graphite armor. (c) Sketch of a divertor pickup cassette. (d) Sketch of a cassette mounted on the divertor baffle and nose. (e) The array of pickups mounted on the center column. Types A, B, and C refer to the dimensions of the pickup coil former, enumerated in Table I.

C. Coil Rogowskis

Rogowski coils are multi-turn coils conceptually similar to pickup coils, except the coil is curved into a loop and used to measure the current the loop encloses. The current supplied to each poloidal field coil of MAST Upgrade is measured by a Rogowski around each coil feed. On MAST-Upgrade, all toroidally flowing currents (including any coil currents or plasma currents) flowing anti-clockwise viewed from above are defined as positive. All PF coils except P1, Px, and Pc are in-vessel coils and, thus, require cases to separate them from vacuum. These coil cases are toroidally contiguous and, thus, can support substantial induced toroidal currents. Therefore, each of these coil cases is enclosed by four separate in-vessel Rogowski coils that measure the sum of coil and case current. These internal coil Rogowskis are secured directly to the coil cases, and the poloidal coordinates of which are available via the MAST-U geometry visualizer.[4] By subtracting the feed current measured by the external Rogowskis (multiplied by the number of coil turns) from the total current measured by the internal Rogowskis, the coil case currents are computed.

D. Plasma current Rogowskis

MAST-U features two types of plasma current Rogwoskis: outer Rogowskis whose path traces the outermost extents of the vacuum vessel (mounted on the vacuum side) and inner Rogowskis whose path takes a shortcut under the divertor tiles, thereby excluding several divertor PF coils. The outer sets of Rogowskis enclose all in-vessel coils, while the inner sets of Rogowskis exclude PF coils D1, D2, D3, and D5. Figure 1 shows the poloidal paths of each Rogowski. In the figure, the Rogowskis are sketched at only one value of toroidal angle but, in fact, they both have an identical set on the opposite side of the machine, 180 toroidal degrees apart (not shown for clarity, since it would obscure the pickup coils). Each of these four Rogowskis is split into four separate segments (inboard vertical, outboard vertical, upper horizontal, and lower horizontal), producing 16 separate signals in total. The total current enclosed by the Rogowskis is computed as a weighted sum of the individual segments whose weights are computed by a calibration procedure described in Sec. III B. The sum of the enclosed coil currents, computed vessel current, and TF pickup is all subtracted from this sum of Rogowski segments to yield the plasma current.

E. Integrators and digitizers

All sensors described here function by the measurement of the voltage induced by a time varying magnetic field and, therefore, require time integration to yield the magnetic flux. Since, in MAST-U, these signals are needed in real-time for use by the plasma control and real-time protection systems, this time integration is performed in hardware. The MAST Upgrade plasma control system is previously reported elsewhere.[8] Two integrator designs are in use on MAST Upgrade, both of which have a 10 kΩ input impedance (chosen to be substantially larger than the probe impedances that are typically less than 10 Ω) and use a 1 μF capacitor for an RC value of 10 ms. The first type outputs a time integrated analog signal that can then be streamed in real-time to the plasma control and real-time protection systems and is separately digitized by a 16 bit digitizer. The second type has an integrated 16 bit digitizer but cannot forward real-time data to downstream users (although this functionality is envisaged for future campaigns to increase the number of signals available to the plasma control system). Digitization, in both cases, has a ±10 V voltage range, which yields a digitization precision of 0.3 mV. For typical calibration factors, this translates to a precision of around 0.3 mT for pickup coils and 0.1 mWb for flux loops, which is far lower than the uncertainty in these probes as calculated in Sec. III.

III. CALIBRATION

The time integrated measurements of flux loops, pickup coils, and Rogowski coils described above all require calibration factors to convert the voltage measurements into Webers (for flux loops), Tesla (for pickups), or Amperes (for the Rogowskis). In MAST Upgrade, all internal magnetics are calibrated *in situ* using the external Rogowskis as references, which are themselves calibrated by the manufacturer to an uncertainty of 0.1%. The external Rogowskis are mounted on the coil feeds and measure the current input into each poloidal field coil. When stationary currents are input into these coils, the static field may be predicted by a DC vacuum code to generate predicted readings of all field sensors. Since all internal probes are calibrated relative to these external Rogowskis, the manufacturer quoted uncertainty value of 0.1% represents the floor of the achievable uncertainty for any internal magnetic diagnostic. In practice, the achieved uncertainty is substantially higher than this, as explained below.

A. Flux loops and pickup coils

The *in situ* calibration procedure for flux loops and pickup coils is as follows. In a dedicated set of vacuum shots, each poloidal field coil is fired separately with a trapezoidal current waveform, which has a sufficiently long flattop to allow all eddy currents to attenuate to negligible levels. Experience has shown 200 ms is sufficient for this, but the flattops are typically on the order of 1 s long. Since induced eddy currents are excluded, predictions of the sensor readings during the stationary flattop can be made with a DC vacuum model. Each probe i has calibration factor α_i, calculated independently of each other. For each of the vacuum shots j, a measurement of the set of $\alpha_{i,j}$ is taken as $\alpha_{i,j} = P_{i,j}/O_{i,j}$, where $P_{i,j}$ and $O_{i,j}$ are the predicted reading (in physics units, T or Wb) and observed reading (in Volts) for probe i and calibration shot j, respectively. The calibration factor for a given probe α_i is then taken as the arithmetic median over calibration shots j. The uncertainty for each α_i is taken as the standard deviation over j. Note that the median over j is used rather than the mean since this measure is more robust to instances where a sensor is particularly close to a specific coil, which can cause small defects in the as-installed position and orientation to be magnified for the vacuum shot in which this coil is fired. To mitigate the effects of high uncertainty probes on downstream calculations (in particular, EFIT reconstructions), probes with calibration uncertainties above a (somewhat arbitrarily chosen) limit are excluded by the inter-shot analysis code. The limits applied in MU01 and MU02 were 0.02 Wb/V for flux loops and 0.2 T/V for pickup coils. The filtered calibration factors and uncertainties are plotted in Fig. 3. After applying this filter, 234 pickup coils (out of 354 total) and 95 flux loops (out of 102 total) remain for analysis. The median

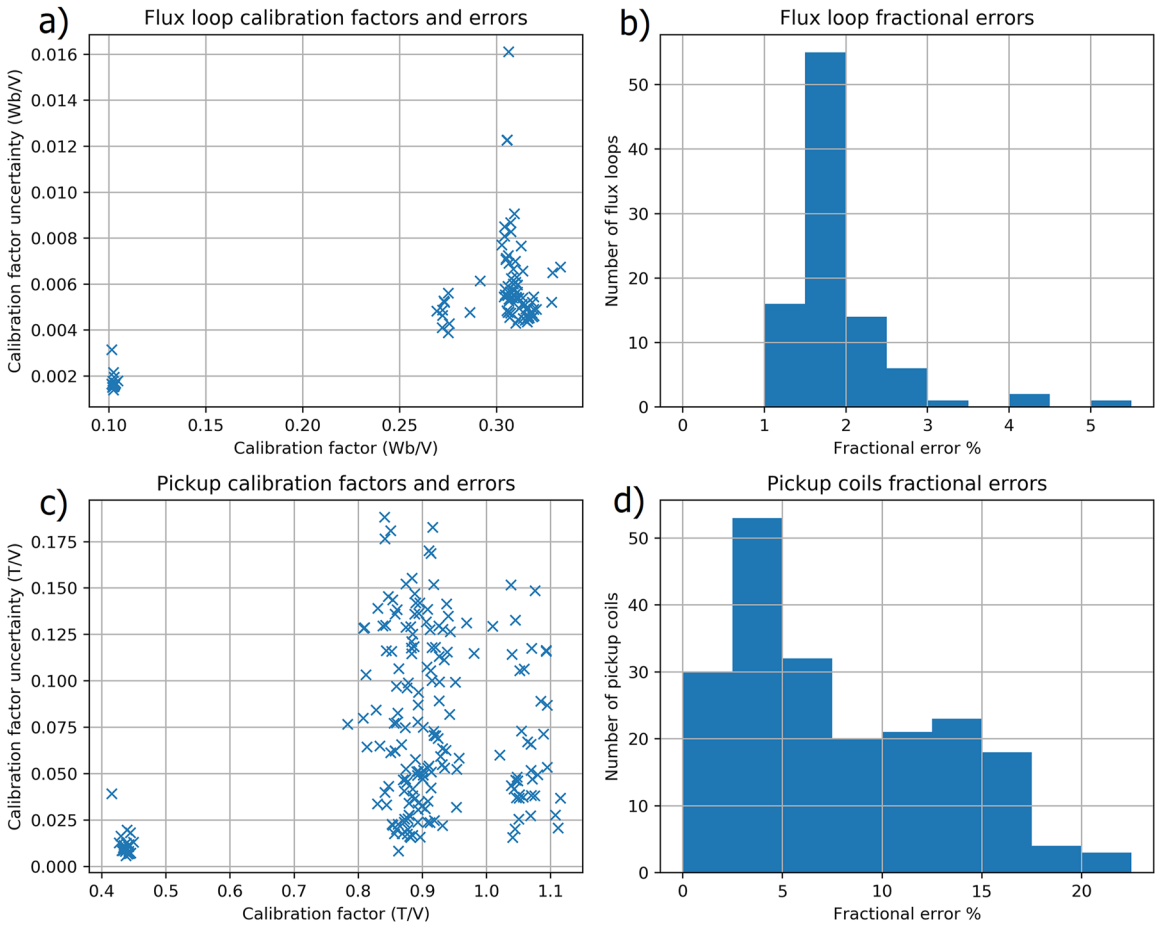

FIG. 3. (a) Calibration factors of the flux loops against their uncertainties. There are two groups on this plot because two types of voltage dividers are applied to the flux loops, which are required to keep the measurements within the integrator voltage rails. (b) A histogram showing the fractional error of the flux loop calibration factor, which indicates the fractional error on the flux loops. The median is 1.7%. (c) Calibration factors of the pickup coils against their uncertainties. These are also in two groups because the center column pickups are summed with their toroidally opposite counterpart prior to integration. (d) A histogram showing the fractional error of the pickup coil calibration factor, which indicates the fractional error on the flux pickup coils. The median is 6.3%. Any probe with a measured uncertainty exceeding 0.2 T/V is excluded from further analysis, and so not included in the above.

uncertainty of the remaining flux loops and pickup coils is 1.7% and 6.3%, respectively. Since flux loops provide a toroidally averaged measurement of a scalar field, they are less sensitive to local irregularities and, therefore, tend to be more accurate than point measurements of a vector field provided by pickup coils, which is reflected in the higher uncertainties of the MAST Upgrade pickup coils. The inter-shot analysis code applies the computed calibration factors to each signal, removes integrator drift and offset, removes TF pickup, and writes the resulting calibrated signals to the MAST-U data archive. It is envisaged that methods for computing probe calibrations and their uncertainties will continue to be refined as the MAST Upgrade program continues, particularly following the processes outlined in Refs. 9 and 10.

B. Plasma current Rogowskis

This same set of vacuum shots is also used to calibrate the plasma current Rogowskis. Because the plasma current Rogowskis do not form a contiguous loop around the poloidal cross section but are instead each comprised of four segments (each producing signal x_k), the measurement of the enclosed current Ip is calculated as a weighted sum of these segments,

$$Ip = \alpha_{Ip}\Sigma_k[\beta_k x_k], \tag{2}$$

where β_k are the segment weights, normalized such that $\Sigma_k\beta_k = 1$. First, the weights β_k are computed by comparing the measured signals from each segment to modeled segments for each vacuum shot. In the same way as the pickups and flux loops are calibrated, each vacuum shot produces an independent measurement of β_k, and the final values are then taken as the median over the vacuum shots. Next the factor α_{Ip} is computed as

$$\alpha_{Ip} = \Sigma[I_c]/\Sigma_k[\beta_k x_k], \tag{3}$$

where $\Sigma[I_c]$ is the sum of the currents of the enclosed poloidal field coils measured by the external Rogowskis. The value and uncertainty

of α_{Ip} are taken as the median and standard deviation over the vacuum calibration shots. This measure yields an uncertainty in the Ip calibration factors of ~3%.

Slight installation defects in all these sensors cause them to also detect a small component of the toroidal field. This TF pickup is measured using a TF vacuum shot, and subtracted prior to application of the calibration factors. In the case of all the diagnostics described here, intershot analysis codes process the raw signals by subtracting TF pickup and integrator drift and applying the computed calibration factors before saving the processed signals for further physics analysis. For example, during MU01, the above set of magnetics diagnostics was used routinely to produce magnetically constrained equilibrium reconstructions using the EFIT++ code, and good agreement with independent diagnostic measurements was demonstrated.[11]

IV. INSTABILITY MAGNETICS

For detecting and diagnosing MHD instabilities, a comprehensive set of instability diagnostics is installed in MAST Upgrade. This consists of three rows of outboard saddle coils and two rows of center column saddle coils, all providing full toroidal coverage. The pickup coils described in Sec. II B may be both collected via an integrator and also digitized separately before integration, allowing these probes to function both as low frequency magnetic field measurements (referred to as pickups) and also high frequency instability sensors (usually referred to as Mirnov coils). Similarly, the saddle coils are digitized as both integrated signals for diagnosing slowly growing instabilities, such as locked modes, and un-integrated signals for diagnosing rapidly rotating global MHD modes. These instability diagnostics are digitized at 200 kHz, which is quite sufficient given that frequencies above this are expected to be attenuated

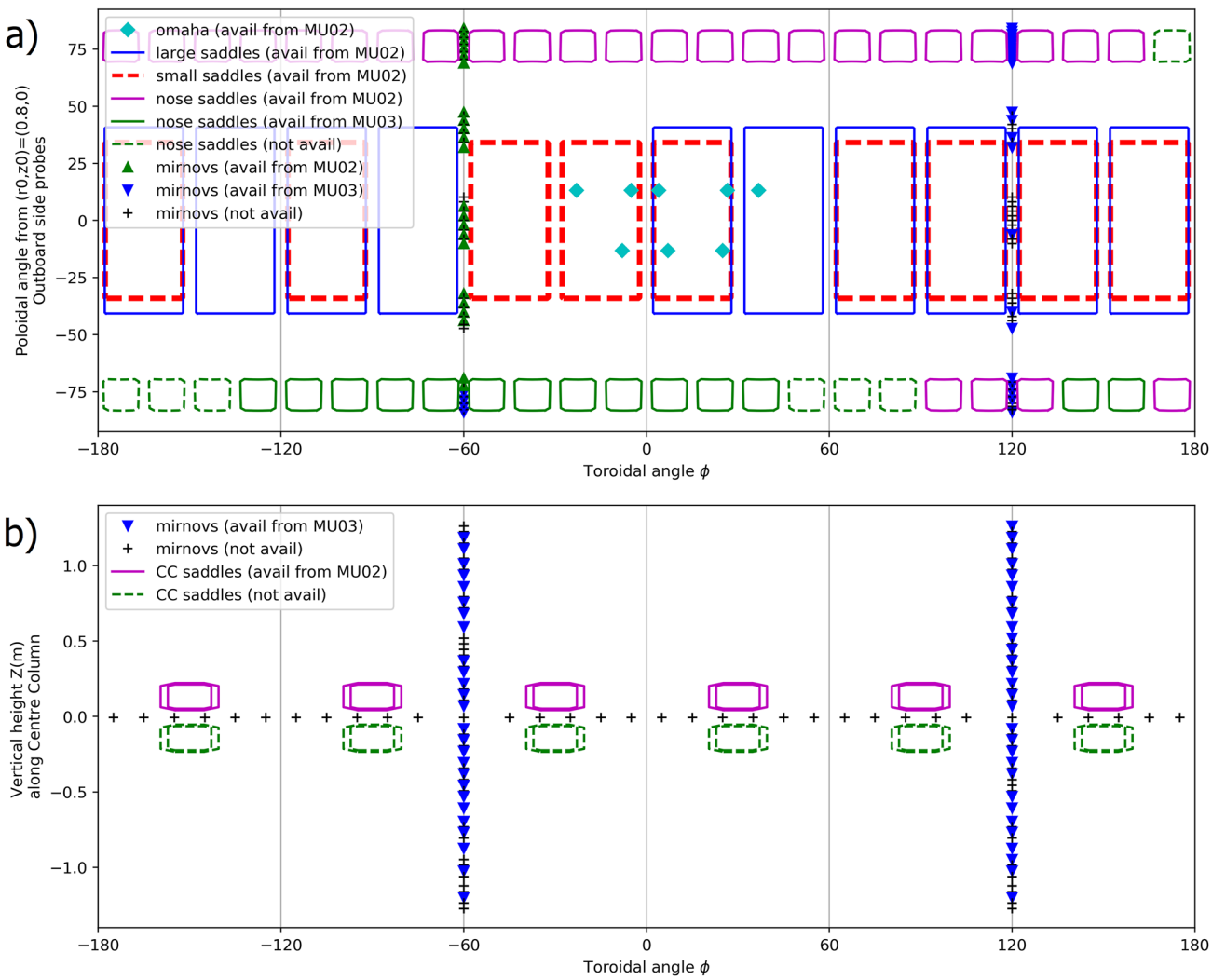

FIG. 4. (a) Sketch of the as-designed 3D sensor locations on the outboard side. Due to insufficient digitization channels, not all the probes can be collected. (b) Sketch of the as-designed 3D sensor locations on the center column. The CC vertical Mirnovs are digitized starting in MU03.

by local vessel armor as described in Sec. II B. The full set of installed instability diagnostics is plotted in Fig. 4. Using the outboard saddle coil toroidal arrays, toroidal mode numbers of detected modes can readily be determined. Figure 5 demonstrates a global MHD mode detected at 11.8 kHz during beam heated discharge 46 445 during MU02. This mode is plainly visible on all the diagnostics plotted in Fig. 4, and therefore, the toroidal mode number can be trivially determined by measuring the rate of change of the phase of the mode with toroidal angle. Due to limited digitizer channels, not all the instability diagnostics plotted in Fig. 4 could be fully commissioned prior to MU02, which made poloidal mode number determination impractical. The installation of an additional digitizer after MU02 has allowed more of the installed Mirnov coils to be added to the poloidal array, greatly extending its poloidal coverage. Therefore, the measurement of poloidal mode numbers of detected modes is anticipated to be routine in MU03, which is scheduled to commence in April 2023.

A. OMAHA coils

The OMAHA diagnostic is an array of Mirnov coils whose frequency characteristics are optimized for the detection of high frequency toroidal modes.[12] In contrast to the other Mirnovs that sit behind thick graphite tiles, the OMAHA coils are protected

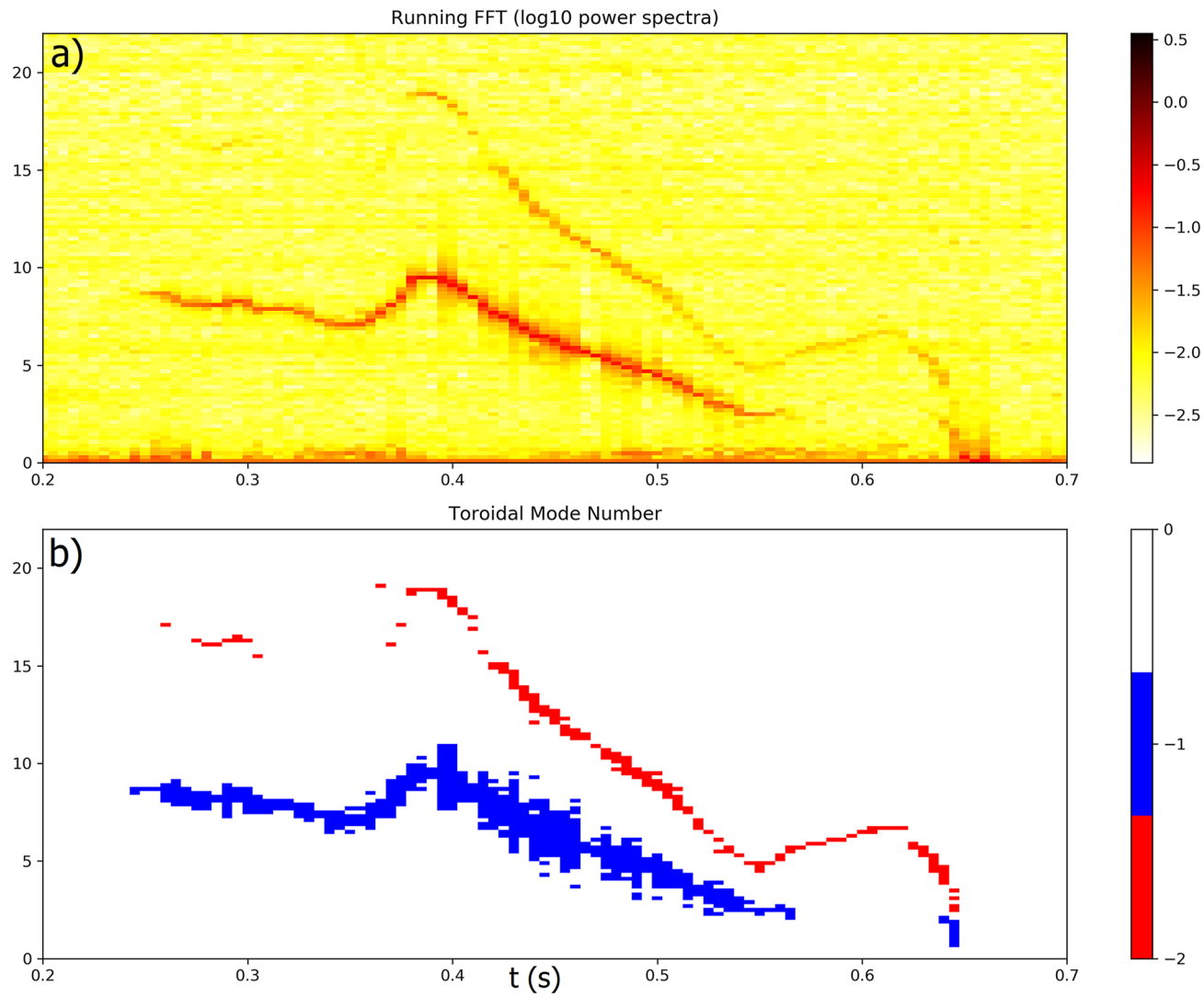

FIG. 5. (a) Frequency spectrogram showing an example global MHD mode in a typical beam heated MAST-U discharge. The physics of this mode are not discussed in this paper, which merely aims to demonstrate their detection and diagnosis. (b) This figure plots the phase of this mode as measured by the outboard saddle coils, against the toroidal angle of the saddle coils, revealing the toroidal mode number of the mode. Global MHD up to 100 kHz is visible on all the commissioned probes and saddle coils sketched in Fig. 4. Having complete toroidal coverage allows ready determination of MHD toroidal mode numbers, as demonstrated here.

by a 3 mm aluminum oxide ceramic sheath coated with a thin layer of colloidal graphite paint. The very high wall frequencies of these protective layers allow these coils to detect frequencies well into the MHz range. Other than slight alterations to their locations they are unchanged from their deployment on MAST, which is described in detail previously.[12] Figure 6 demonstrates a typical target mode for the OMAHA coils; in this case, an Alfven Eigenmode at around 2 MHz was used. Toroidal mode number determination is also possible using the OMAHA array, but this is not performed here.

V. DISCUSSION AND OUTLOOK

This paper describes the current state of the Mast Upgrade magnetic diagnostics just prior to the third campaign. While very far from matured, they have provided vital machine and plasma

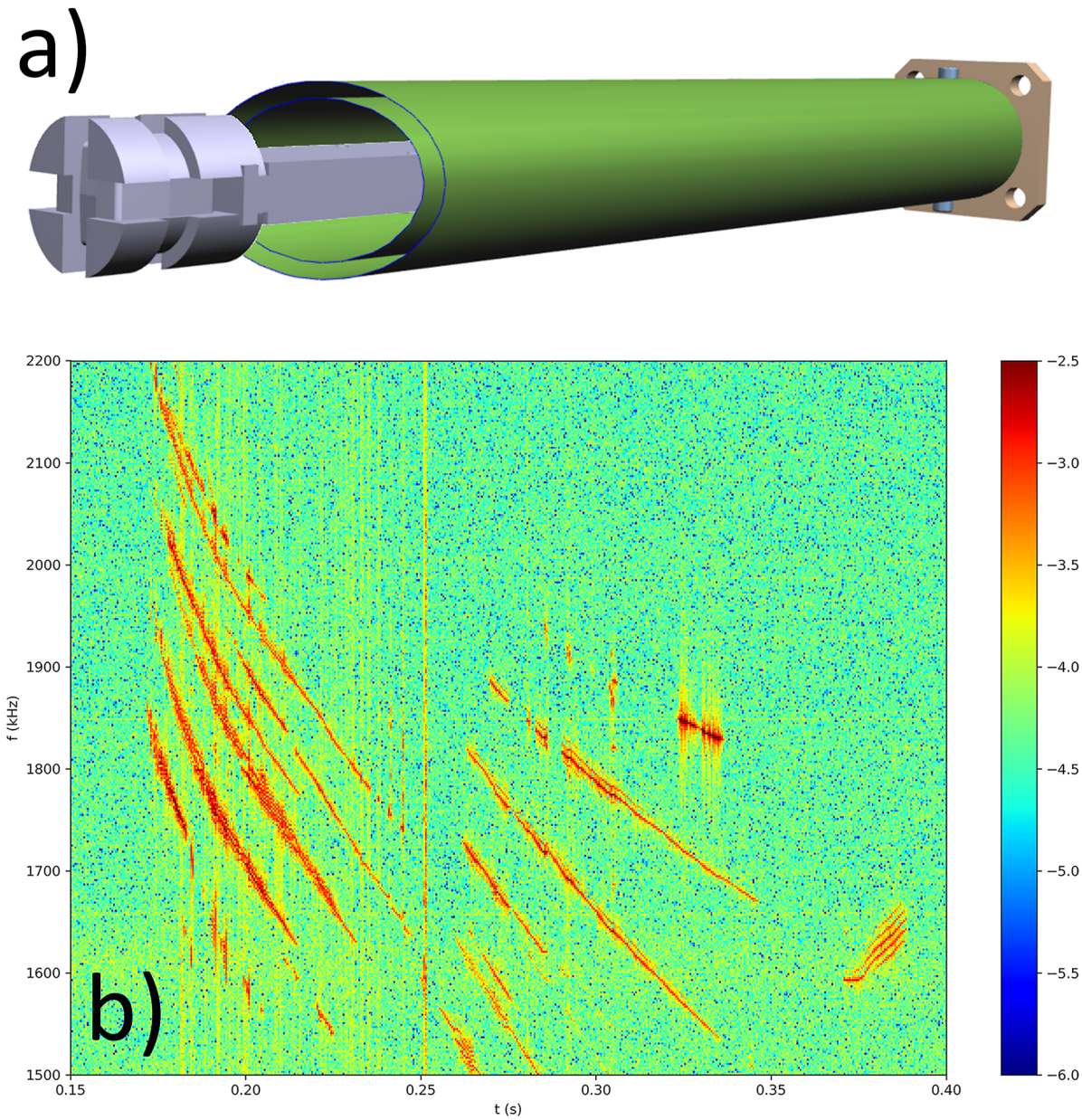

FIG. 6. (a) Sketch of an OMAHA probe. The bobin on the end supports three coils, wound to measure three orientations separately. The ceramic cover and thin graphite paint armor have a negligible shielding effect allowing frequencies in the MHz range to be measured. (b) An example of a target mode around 2 MHz from a typical beam heated MAST-U discharge.

information to facilitate the first campaigns, notably facilitating equilibrium reconstructions that agree well with independent diagnostics, as well as reliably providing essential signals for plasma control, and for basic machine operation and protection. Nonetheless, the progress reported here represents only the start of the development of the MAST Upgrade magnetic diagnostics, all aspects of which have significant scope for improvement. Most notably, the calibration procedures used in the initial MAST Upgrade campaigns are, in general, over-simplistic and should be brought in line with modern rigorous standards, following Ref. 10.

During MU02, there were insufficient digitizer channels to collect all the instability diagnostics, making the determination of poloidal mode numbers of detected MHD modes impractical. During the engineering break prior to MU03, the poloidal coverage of the Mirnov coil array has been extended (specified in Fig. 4) to facilitate the diagnosis of the poloidal mode numbers of detected MHD modes. This facility is expected to be employed routinely in MU03, commencing in April 2023. Currently, the saddle coils are all integrated and digitized individually, so the measured signal is dominated by the n = 0 equilibrium component, making it difficult to extract higher n slowly varying 3D fields such as those of interest to RMP plasma response studies.[13] It is envisaged that, in the future, the outboard saddle loop array will be reconfigured as a set of differenced pairs following Ref. 14, such that slowly varying fields may be accurately diagnosed.

The median uncertainty in the calibration factors of the flux loops is 1.7%, which is considered adequate. However, the accuracy may be improved further following Ref. 10 by subtracting a reference flux loop in hardware to eliminate the contribution of the central solenoid to improve the dynamic range of the flux loop array.

Of the 354 poloidal field pickup coils installed in MAST Upgrade, only 234 (65%) are routinely used in the first campaigns, mostly due to the uncertainty of their calibration factor exceeding the limit of 0.2 T/V, which was applied to limit the uncertainty in data entering the analysis stream. Of these that remain, the median calibration uncertainty is 6.3% but can range up to 15%–20%, which is considered wildly excessive and should be urgently addressed in future works. To generate the predicted readings used in the calibration procedure, accurate and precise knowledge of the location and orientations of each probe relative to the PF coils is required, and therefore, small deviations between the as-designed and as-built sensors and PF coils can result in substantial errors in the probe calibrations. It is envisaged that these errors may be reduced by an optimization procedure that minimizes the calibration error by slightly varying the simulated probe locations and orientations to better reflect their likely as-built counterparts, as in Ref. 9. This procedure would increase the utility of the MAST Upgrade pickup coil arrays by reducing the calibration uncertainties. Also, any detected correlation between locations of high error probes and particular poloidal field coils would yield information on the deviations from axi-symmetry in the poloidal field, which would assist error field studies.

The *in situ* calibration procedure ultimately derives calibration factors from the external Rogowski calibration factors, so all magnetic calibrations share a dependency on the external Rogowski coil calibration. Having a separate and independent measure of the magnetic field would, therefore, be of great value to the MAST Upgrade magnetics system and eliminate this single dependency, and options for providing this are being explored.

ACKNOWLEDGMENTS

This work was funded by RCUK Energy Program (Grant No. EP/W006839/1).

AUTHOR DECLARATIONS

Conflict of Interest

The authors have no conflicts to disclose.

Author Contributions

D. A. Ryan: Data curation (lead); Formal analysis (lead); Investigation (lead); Methodology (lead); Software (lead); Validation (lead); Visualization (lead); Writing – original draft (lead); Writing – review & editing (equal). **R. Martin**: Conceptualization (equal); Funding acquisition (equal); Project administration (equal); Supervision (lead). **L. Appel**: Writing – review & editing (equal). **N. B. Ayed**: Investigation (equal); Methodology (equal). **L. Kogan**: Validation (equal). **A. Kirk**: Conceptualization (equal); Funding acquisition (equal); Validation (equal).

DATA AVAILABILITY

To obtain further information on the data and models underlying this paper please contact PublicationsManager@ukaea.uk.

REFERENCES

[1] M. Cox, Fusion Eng. Des. **46**, 397–404 (1999).
[2] T. Edlington *et al.*, Rev. Sci. Instrum. **72**, 421–425 (2001).
[3] J. R. Harrison *et al.*, Nucl. Fusion **59**, 112011 (2019).
[4] UKAEA, MAST-U geometry visualiser, 2023, https://users.mastu.ukaea.uk/internal/mastu-visualiser (accessed 06 July 2023).
[5] The Quadrant Group, Ketron 1000 PEEK technical data sheet, 2011, https://www.theplasticshop.co.uk/plastic_technical_data_sheets/peek_1000_technical_data_sheet.pdf (accessed 03 February 2023).
[6] J. W. Berkery *et al.*, Plasma Phys. Controlled Fusion **63**, 055014 (2021).
[7] J. D. Huba, NRL PLASMA FORMULARY Supported by The Office of Naval Research, Naval Research Laboratory, Washington, DC, 2013.
[8] G. McArdle *et al.*, Fusion Eng. Des. **159**, 111764 (2020).
[9] J.-M. Moret *et al.*, Rev. Sci. Instrum. **69**, 2333–2348 (1998).
[10] E. J. Strait, Rev. Sci. Instrum. **77**, 023502 (2006).
[11] L. Kogan *et al.*, "First MAST-U equilibrium reconstructions using the EFIT++ code," in *Proceedings of the 48th EPS Conference on Plasma Physics* (European Physical Society, Maastricht, 2022), pp. 2–5.
[12] M. J. Hole *et al.*, Rev. Sci. Instrum. **80**, 123507 (2009).
[13] S. Munaretto *et al.*, Phys. Plasmas **25**, 072509 (2018).
[14] S. Munaretto *et al.*, Rev. Sci. Instrum. **92**, 073504 (2021).